

188  
2-1-77

Dr 634  
UCRL-50025-76-3

## ELECTRONICS ENGINEERING DEPARTMENT QUARTERLY REPORT NO. 3 - 1976

Inside: Versatile gamma-ray spectrometer operates almost anywhere  
Electronic corrector bar boosts precision of NC machine tool  
New x-ray spectrometer provides fast results for laser experiments  
Pockels cells find new applications in advanced laser systems

MASTER

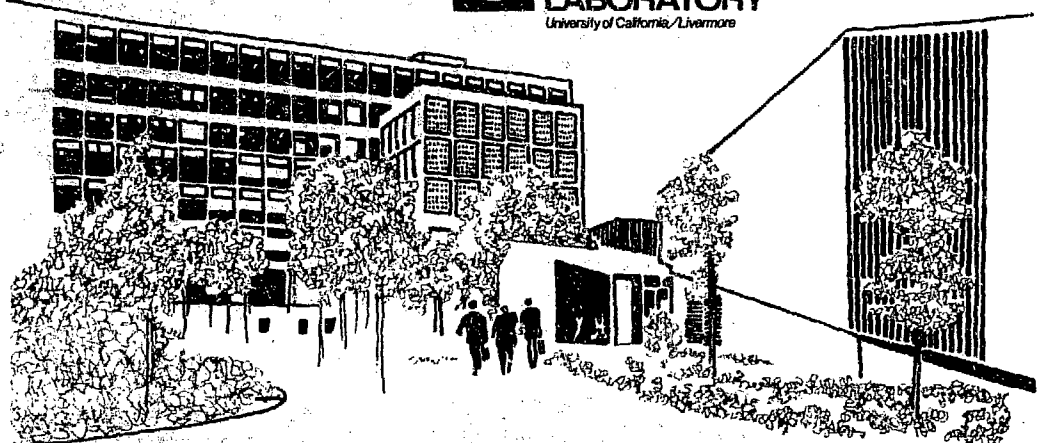
October 8, 1976

Prepared for U.S. Energy Research & Development  
Administration under contract No. W-7405-Eng-48



LAWRENCE  
LIVERMORE  
LABORATORY

University of California/Livermore



DISTRIBUTION OF THIS DOCUMENT IS UNLIMITED

### NOTICE

This report was prepared as an account of work sponsored by the United States Government. Neither the United States nor the United States Energy Research & Development Administration, nor any of their employees, nor any of their contractors, subcontractors, or their employees, makes any warranty, express or implied, or assumes any legal liability or responsibility for the accuracy, completeness or usefulness of any information, apparatus, product or process disclosed, or represents that its use would not infringe privately-owned rights.

### NOTICE

Reference to a company or product name does not imply approval or recommendation of the product by the University of California or the U.S. Energy Research & Development Administration to the exclusion of others that may be suitable.

#### Printed in the United States of America

Available from

National Technical Information Service  
U.S. Department of Commerce  
5285 Port Royal Road  
Springfield, VA 22161

Price: Printed Copy \$ ; Microfiche \$3.00

Page Range	Domestic Price	Page Range	Domestic Price
001-025	\$ 3.50	326-350	10.00
026-050	4.00	351-375	10.50
051-075	4.50	376-400	10.75
076-100	5.00	401-425	11.00
101-125	5.50	426-450	11.75
126-150	6.00	451-475	12.00
151-175	6.75	476-500	12.50
176-200	7.50	501-525	12.75
201-225	7.75	526-550	13.00
226-250	8.00	551-575	13.50
251-275	9.00	576-600	13.75
276-300	9.25	601-up	*
301-325	9.75		

\*Add \$2.30 for each additional 100 page increment from 601 to 1,000 pages;  
add \$4.50 for each additional 100 page increment over 1,000 pages.



**LAWRENCE LIVERMORE LABORATORY**  
*University of California, Livermore, California 94550*

UCRL-50025-76-3

**ELECTRONICS ENGINEERING DEPARTMENT  
QUARTERLY REPORT NO. 3 — 1976**

MS. date: October 8, 1976

## **Foreword**

The EE Department Quarterly Report is published with two purposes in mind: (1) to inform readers of various activities within the Department, and (2) to promote the exchange of ideas.

The articles, by design, are brief summaries of EE work. For further details on a subject covered, please contact the individual listed at the beginning of the article in question; that person is primarily responsible for the content of that article. Inasmuch as most projects are the result of the cooperative efforts of many individuals, the article contact may either provide the requested information directly or refer you to the appropriate person to answer your question.

EE Department personnel are encouraged to submit articles for consideration to the Publications Committee. Committee members include:

- B. D. Faraldo -- Field Test Systems Division
- V. R. Latorre -- Engineering Research Division
- G. P. Ledbetter -- Technical Editor
- S. A. Nielsen -- Operations Division
- T. J. Nugent -- Chemistry and Computation Systems Division
- W. F. Thompson -- EE Department Staff
- G. E. Voglin -- Fusion Energy Systems Division
- S. D. Winter -- Nuclear Energy Systems Division

## Contents

EE's Gamma-Ray Spectrometer Answers the National Need for a Portable, Rugged, Self-Contained Radioisotope Analyzer . . . . .	1
With the Help of a Microcomputer-Based Error Correcting System, a Numerically Controlled Machine Tool Achieves Precision Well Beyond Its Normal Mechanical Limits . . . . .	7
A New X-Ray Spectrometer Provides the Recording Speed Needed to Analyze Electron Temperatures and Densities in Laser-Induced Plasmas . . . . .	12
New Developments in Electrooptic Modulator Technology Have Created Specialized Pockels Cells That Meet the Demanding Requirements of Laser Systems . . . . .	19

# EE'S GAMMA-RAY SPECTROMETER ANSWERS THE NATIONAL NEED FOR A PORTABLE, RUGGED, SELF-CONTAINED RADIOISOTOPE ANALYZER

Growing national interest in public safety has produced a sudden need for a type of radiation-monitoring equipment that doesn't exist anywhere commercially. An easily portable, very rugged, and completely self-contained instrument is required that can be set up quickly and virtually anywhere to detect and identify radioactive isotopes. The Electronics Engineering Department has responded to this need by designing and developing the first equipment that can fulfill all these requirements. This instrument, a 1024-channel gamma-ray spectrometer, has already gone into limited production to provide health physicists at LLL and other Energy Research and Development Administration (ERDA) laboratories with an effective tool for monitoring possible sources of radioactivity.

## Introduction

Health physicists and others who are involved in general environmental monitoring, or who must be capable of responding quickly and flexibly during an emergency, are increasingly hampered by certain limitations present in all available radioisotope-measuring equipment. Such persons need equipment that can be carried practically anywhere and operated by a single individual; the equipment should be simple to operate, since the user may not be a trained technician. The required instrument must be capable of making sophisticated measurements, and yet it must be very lightweight and compact. It must operate reliably under a wide range of weather conditions including extreme cold or heat, rain, wind, and dust. It must not rely on local electrical power or other equipment in order to operate.

Until the EE Department introduced its prototype gamma-ray spectrometer in 1974, such an instrument didn't exist. The prototype has since undergone further development and refinement to the point where a second-generation instrument has been built in limited quantities and sold to other ERDA laboratories.

The recent interest shown in the EE instrument by commercial manufacturers suggests that LLL's success in this project and the ready availability within the public domain of all details of the design will soon encourage the appearance of commercially made equipment on a large scale.

---

*For further information on this article, contact Alan L. McGibbon (Ext. 5073).*

## Identifying Radioactive Isotopes

Radioisotopes spontaneously emit radiation in the form of a number of subatomic particles (alpha particles, beta particles, and neutrons) and electromagnetic radiation (x rays and gamma rays). Each radioisotope produces radiation in characteristic patterns that can be used to identify it. Therefore, if we can build a detector that recognizes each pattern, we have the basis for an instrument that can detect and identify unknown radioisotopes.

In practice, the characteristic pattern of emitted gamma radiation is sufficient to identify each radioisotope. This is convenient, since gamma rays, which possess higher energy than x rays, have good penetration characteristics and tend to pass more completely through solid objects. This characteristic makes the case of our radioisotope analyzer transparent to gamma rays, and it allows us to leave the detector inside the case. The gamma rays involved in these measurements usually range in energy from about 100 keV to 3 MeV.

## The Gamma-Ray Detector

Gamma-ray detectors operate on a simple principle. The passage of gamma radiation into a detector creates an electrical pulse whose charge is proportional to the energy lost by the gamma rays. This is commonly done by allowing the gamma rays to pass through a crystal that possesses the special property of emitting light at an intensity directly proportional to the energy of the gamma rays. The light from the crystal passes into a photomultiplier tube, where electric pulses are produced whose charges vary with the intensity of the light.

Detectors using a sodium iodide crystal are widely used because of their low cost and ease of use. Another detector that uses a relatively pure germanium crystal has better resolution, but it may cost as much as \$10 000, and it requires very low-temperature cooling during operation. The sodium iodide detector is the main detector used with the LLL gamma-ray spectrometers, although we have had a private company design a germanium detector that may also be used externally.

## Measuring the Gamma-Ray Energies

During the identification of a radioisotope, the height of each voltage pulse from an amplifier following the detector is measured and stored in a

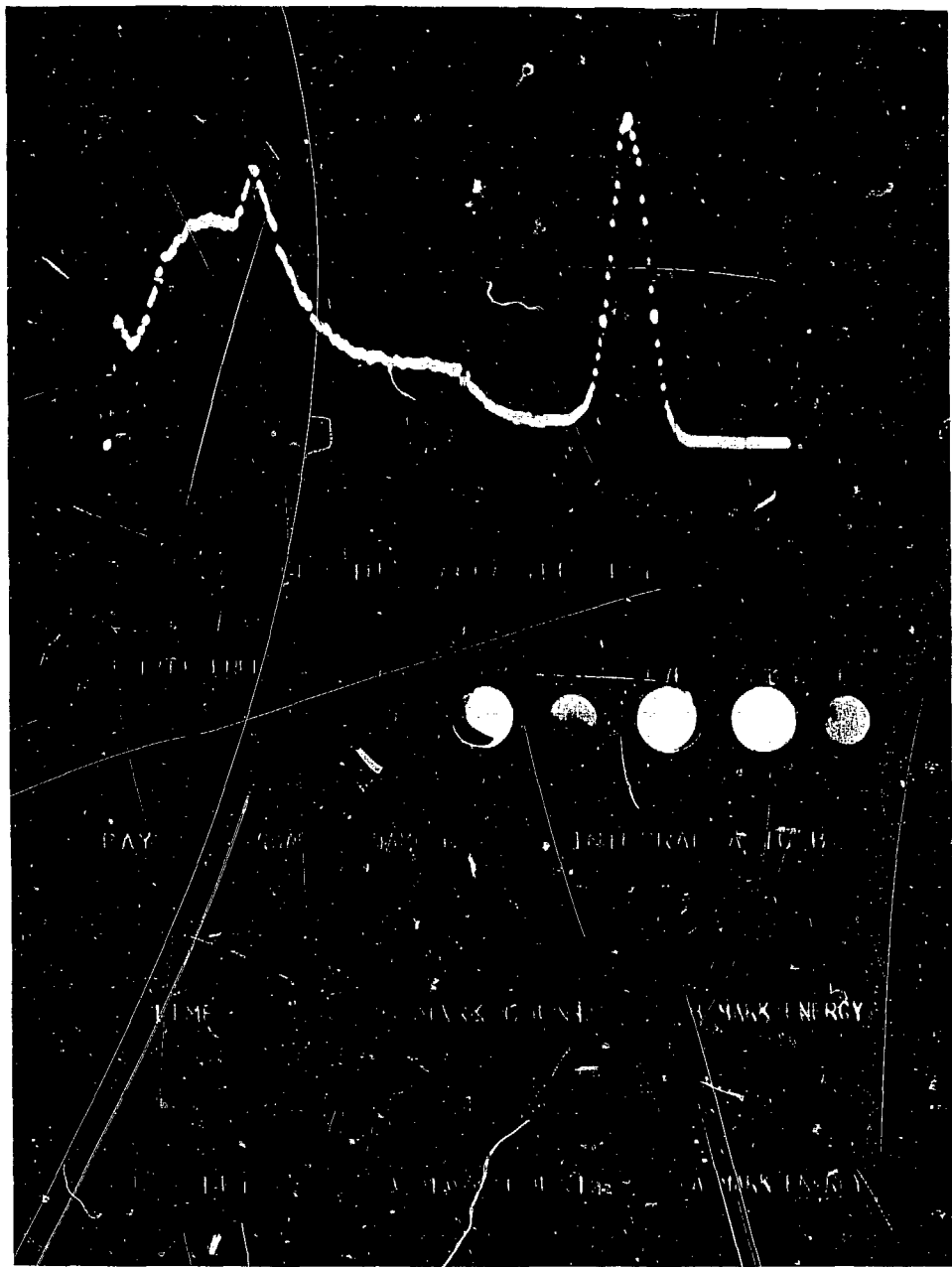


Fig. 1. Photograph of the display produced by the gamma-ray spectrometer. The curve at the top is a 256-point plot of counts vs memory locations. The LED's immediately below the curve display useful information that can be photographed with each plot to provide a complete record.

memory. Different locations in the memory represent all the possible pulse heights. As each pulse is measured, the count in the memory location representing that pulse height is incremented by one count.

After a period of time has elapsed and a number of pulses have been measured, a plot of memory counts vs memory locations is made on a cathode-ray tube (CRT). An example is shown in Fig. 1. This plot of counts vs memory locations is proportional to counts vs voltage pulse heights for the same period of elapsed time, which, after an energy calibration, is in turn proportional to counts vs energy in the gamma-ray spectrum. From the peaks on such a plot, a health physicist can easily determine which radioisotopes are present in a sample.

#### **Features Needed on the Spectrometer**

In order for the spectrometer to be a truly useful instrument, its design must include a number of features besides its basic ability to detect radioisotopes and display their energy spectra. First, it should be capable of reading out the energy of peaks in keV units and the counts for that energy. Sometimes the integration of a peak is needed, and it must be easy to set limits and read out the results. It should be possible to record several spectra in succession, to compare them against each other, and to add or subtract from them.

Record-keeping data, such as time of day and sample number, should be read out and displayed along with all the other parameters and spectra, so that a recording camera may photograph all the information simultaneously (see Fig. 1). A digital-information storage medium, such as magnetic tape, would also be useful for recording all the information.

#### **The First-Generation Spectrometer**

In 1973, LLL designed and constructed the prototype instrument, a 256-channel gamma-ray spectrometer. The term 'channel' refers to the number of memory locations used. In this first instrument the spectrum viewed in the CRT display was divided into 256 equal increments of energy. The resulting curve was made up of 256 dots.

The prototype machine had sufficient memory for one spectrum, and it could integrate and do a background subtraction approximation based on a straight line drawn between the two points to be integrated. It had two movable markers on the displayed energy-spectrum curve, one of which read out directly in keV energy units. The time of day, day of the year, and sample number, together with peak energy, the integral, live elapsed time, and preset live time were all displayed on light-emitting diodes

(LED's) near the CRT so that the instrument's polaroid camera could record the curve and all important digital information at one time. The spectrometer would operate for 8 h on its internal rechargeable batteries, and it was completely self-contained in a waterproof aluminum case.

The spectrometer was operated using its 24-button keyboard. The keyboard minimizes knob turning, which may be difficult if an operator must wear gloves in a cold climate.

The detector included a 50-mm  $\times$  50-mm sodium iodide NaI(Tl) crystal and a photomultiplier, both mounted in shock- and temperature-insulating foam and housed in a protective well along the side of the instrument. The detector could be used in place, or it could be removed and hung on a tripod that was carried in the cover of the instrument.

The digital logic of the instrument consisted of 300 medium-scale integrated (MSI) circuits of the complementary metal oxide semiconductor (CMOS) type. This is equivalent to approximately 10 000 transistors.

#### **The Second-Generation Spectrometer**

The second-generation portable gamma-ray analyzer provides features not available in the prototype instrument. Compared to the prototype, which was a one-of-a-kind instrument, the second-generation spectrometer is a well-packaged, easily accessible unit (see Fig. 2). It can digitize and store one 1024-channel spectrum or four 256-channel spectra. The 256-channel spectra may be moved, added, or subtracted. Integration is available, as before. The display is larger, consisting of 46 characters of LED information, 6 status indicators, and the same 50-mm  $\times$  75-mm cathode-ray tube for plotting (refer again to Fig. 1). The entire display can be photographed by an automatically controlled Polaroid SX-70 camera. The data can also be telemetered out in a teletype ASCII format using a 1200- and 2200-Hz voltage-controlled oscillator (VCO). This allows the data to be recorded on a conventional audio tape recorder or sent over ordinary telephone lines to a remote viewer or computer (see Fig. 3). A 36-button keyboard allows many more analyzing, computing, and display features than the first instrument possessed. Some of the features are:

- Either linear or logarithmic displays can be made.
- Data acquisition can be programmed to stop on overflow, preset time, preset counts, or preset counts in a specific channel.
- Three markers read out in energy, and two of them also read out in counts.
- Pushbutton control is provided in binary steps for amplifier gain, which is also read out on the display.



Fig. 2. The gamma-ray spectrometer being used in the field. Here the spectrometer is being operated by following the easy instructions printed inside the cover.

- The energy scale can be offset up to 50% of full scale (i.e., 1 MeV to 2 MeV on the display).
- The vertical CRT scale can be expanded or compressed by pushbutton control.
- Two spectra can be overlapped on the CRT.
- The display conserves power by turning itself off when it's not in use.
- A blinking warning light on the display indicates that the operator has typed in an invalid or incomplete command.

### Electronics

The second-generation instrument will run for 10 to 20 h on rechargeable gel cell batteries, which can be removed and replaced easily in emergencies. The digital logic is contained in 500 CMOS MSI circuits configured into a 32-bit, special-purpose computer design. Five controllers provide most of the mathematical operation, while several other controllers handle peripherals such as LED multiplexing, CRT plotting, time keeping, and marker moving.

The time-of-day plus day-of-the-year clocks are run continuously off the batteries so they won't lose time while the spectrometer isn't in use. The memory and all important registers are controlled by a

memory-protect switch; if the spectrometer is operated with the switch on, memory will be saved for several months.

Although the instrument does not use a microprocessor (which wasn't available in CMOS soon enough), the logic and flow charts can be converted to a microprocessor in later designs to conserve chip space and save weight.

The preamplifier and analog-to-digital converter (ADC) are low-power designs using operational amplifiers. The ADC runs at 8 MHz and is of the Wilkinson type. All linear circuitry is designed to provide negligible drift over a 100°C operating temperature range (-30 to +70°C). Six peripheral printed circuit boards and a special wire-wrap plane (shown in Fig. 4 and discussed in the next section) are all designed for high reliability using the best of components. All circuitry is designed to draw minimal power. An example of this is the use of a converter to change the 12 V battery voltage to 5 V to run the light-emitting diodes. Overall, this saves 50% in power to the lamps. The logic runs from regulated +10 V battery power, while the linear circuitry uses  $\pm 12.250$  V from a dc/dc converter and a dual high-stability regulator. An internal, 1 kV regulated supply is present for the shock-mounted NaI(Tl) detector, which is carried in a front panel well, similar to that located on the side of the prototype model.

### Mechanical Design

The analyzer package is functional, environmentally protected, and esthetic. The overall shape resembles a piece of luggage for ease of transportation. The waterproof cover can house either a standard Polaroid SX-70 camera and accessories or a SONY TC55 tape recorder and accessories. With the cover removed, the front panel is splash-proof and can be hosed down to remove salt if the instrument has been used in a salt-spray environment. All exposed metals have been plated to resist corrosion, and all switches and controls are sealed. An additional waterproofing cover encloses the recessed front panel to protect more controls and the detector, which are less watertight and are rarely adjusted.

Normal operation requires only the use of the keyboard and three CRT display knobs below the display bezel. Recessed panel adjustments allow fine adjusting of amplifier and ADC, and access to the memory-protect switch, high-voltage switch, time-setting switch, and telemetry output jack. Other jacks are provided here for using other detector types.

The case is built of polypropylene and aluminum. Most internal chassis parts are made from hydroformed aluminum; other parts are machined aluminum or polycarbonate. Metal parts are connected by riveting



Fig. 3. The spectrometer coupled to a telephone for data transmission. The Polaroid camera is shown in place over the display window.



**Fig. 4.** The folding wire-wrap plane containing most of the digital logic. The six boards are shown unfolded here for a better view.

and epoxy bonding. Lock screws are used only for removable components of the chassis.

The edge-lit display legend/graticule allows the legend information to be photographed. The legend is engraved in the scratch-resistant polyallyldiglycol carbonate graticule using a Gerber computer plotter with a diamond stylus.

Most of the digital logic is mounted on a unique six-board, folding wire-wrap-plane system to eliminate connectors (refer to Fig. 4). The six 127-mm X 203-mm (5-in. X 8-in.) boards are held together with polypropylene hinges and unfold to about 1 m (40 in.). When folded, they occupy 127 mm X 203 mm X 203 mm and hold 500 integrated circuits.

The complete spectrometer, containing batteries, line cord for 115/230 V, 50/60 Hz operation, Polaroid camera, camera mount for automatic photo making, viewing hood for bright sunlight, NaI detector, and cables weighs 16 kg (35 lb).

#### **Acknowledgments**

This project was conceived by members of the Hazards Control Department at LLL. The Mechanical Engineering Department designed the chassis parts and the carrying case to meet our requirements.

# WITH THE HELP OF A MICROCOMPUTER-BASED ERROR CORRECTING SYSTEM, A NUMERICALLY CONTROLLED MACHINE TOOL ACHIEVES PRECISION WELL BEYOND ITS NORMAL MECHANICAL LIMITS

The production of optical-quality surfaces for laser mirrors demands machining accuracies that are beyond the mechanical limits of even the best numerically controlled (NC) machine tools. Deviations from a true straight line as major machine parts slide along their axes produce consistent, repeated machining errors. An NC machine tool at LLL has been modified so these errors are compensated for by an 'electronic corrector bar' containing an MCS-80 microprocessor and an associated look-up table. The new system computes the positions of machine parts as they move along their axes, finds the appropriate corrections in the look-up table at each 254  $\mu\text{m}$  (0.010 in.) (10 mil) of part travel, and issues positional correction commands. The 'electronic corrector bar,' which could be used with many other NC machine tools, has reduced this machine's positional error from 1.5  $\mu\text{m}$  (60  $\mu\text{in.}$ ) to 0.1  $\mu\text{m}$  (5  $\mu\text{in.}$ ) and its straightness error from 0.6  $\mu\text{m}$  (25  $\mu\text{in.}$ ) to 0.1  $\mu\text{m}$  (5  $\mu\text{in.}$ ) — providing the greater precision needed to machine laser mirrors.

## Introduction

New demands for ever greater precision are placed on machine tools each year. The advent of numerical control (NC) has eliminated human error from precision machining, and mechanical refinements have carried us to the point where further accuracy seems impossible. Nevertheless, new demands continue to be made.

Such a demand was made at LLL when a machine tool was given the task of doing the exceedingly precise machining required to figure the optical surfaces of laser mirrors. The machine chosen for the task was a Moore diamond turning machine under the control of a very accurate NC system. While this configuration alone couldn't possibly provide the required accuracy, it could be combined with an 'electronic corrector bar' that automatically sends information to the NC system to correct for minute inaccuracies in the machine's movements. This has been done, and it works well.

## Numerical Control of Machine Motions

The diamond turning machine does its work by means of motions along three machine axes,

represented schematically in Fig. 5. The part being machined (the laser mirror) rotates about the horizontal spindle. The diamond tool moves toward and away from the mirror along the horizontal Z-axis and across the face of the mirror along the horizontal X-axis.

The NC system controls all motions about the C-axis and along the X- and Z-axes. For example, motion of the diamond tool along the X-axis is controlled by the command loop shown in Fig. 6. The preprogrammed NC instructions are read from punched paper tape and converted to a velocity command voltage that is sent from the controller to a servo drive. The servo turns a leadscrew, which moves a machine table holding the diamond tool. To confirm that the proper motion has taken place, the movement of the leadscrew is detected by a resolver, which sends feedback signals to the controller. The feedback signals are compared with the command signals, and if they differ, velocity voltages will be sent to the servo to drive the position errors to zero.

## Unavoidable Machine Errors

Here, then, is the basic NC machine tool — very accurate, but not accurate enough for the task at hand. The problem is that even the finest machine tool is not ideally capable of perfectly straight movement. Consider the motion of the diamond tool once again as it moves along the Z-axis. Figure 7 is a view from above the tool looking straight down the C-axis. We see three geometrical errors. There may be a positional error along the Z-axis. There may be a straightness error — a linear displacement perpendicular to the Z-axis. And there may be a squareness error — an angular displacement between the Z-axis and the X-axis.

The one good thing about these three errors is that they repeat very nicely; the same errors occur to the same extent each time the table carrying the tool reaches the same position. One of these errors, the positional error, can be corrected partially by a clever device called a mechanical corrector bar, which capitalizes on the error's repeatability. The bar rotates the machine's feedback resolver slightly according to the machine's position along one of the machine axes. While the result is a distinct improvement, even the positional accuracy still isn't good enough, and the

*For further information on this article, contact Howard A. Whelan (Ext. 5133).*

straightness and squareness errors remain completely uncorrected.

#### **Solution: the Electronic Corrector Bar**

The problem of the three unavoidable errors was solved by the introduction of LLL's 'electronic corrector bar' (analogous to the mechanical corrector bar) into the system. This corrector consists of an MCS-80 microprocessor whose programmable read-only memory (PROM) contains a corrector program and a correction look-up table. The look-up table contains a correction 'word' for each 254  $\mu\text{m}$  (10 mil) of travel along a machine axis. Each correction word contains positional, straightness, and squareness corrections. The data for these corrections were gathered by taking error measurements with a laser interferometer at each 254- $\mu\text{m}$  position.

The corrector monitors machine position along an axis by counting the command pulses within the NC controller. At each 254- $\mu\text{m}$  interval, the corrector selects the proper correction word from the look-up table and distributes the corrections at each 13- $\mu\text{m}$  (1/2-mil) position over the next 254  $\mu\text{m}$  of travel. The corrections are made by converting the correction word into pulses that are inserted into the regular stream of command pulses in the NC controller.

In theory, the correction pulses from the corrector could be inserted either into the NC system's stream of command pulses or into its feedback signal. In this particular application only the first method was possible, since the feedback signal is produced by a resolver, which doesn't produce a signal consisting of pulses. Generally speaking, the electronic corrector bar can be incorporated into any NC control system that

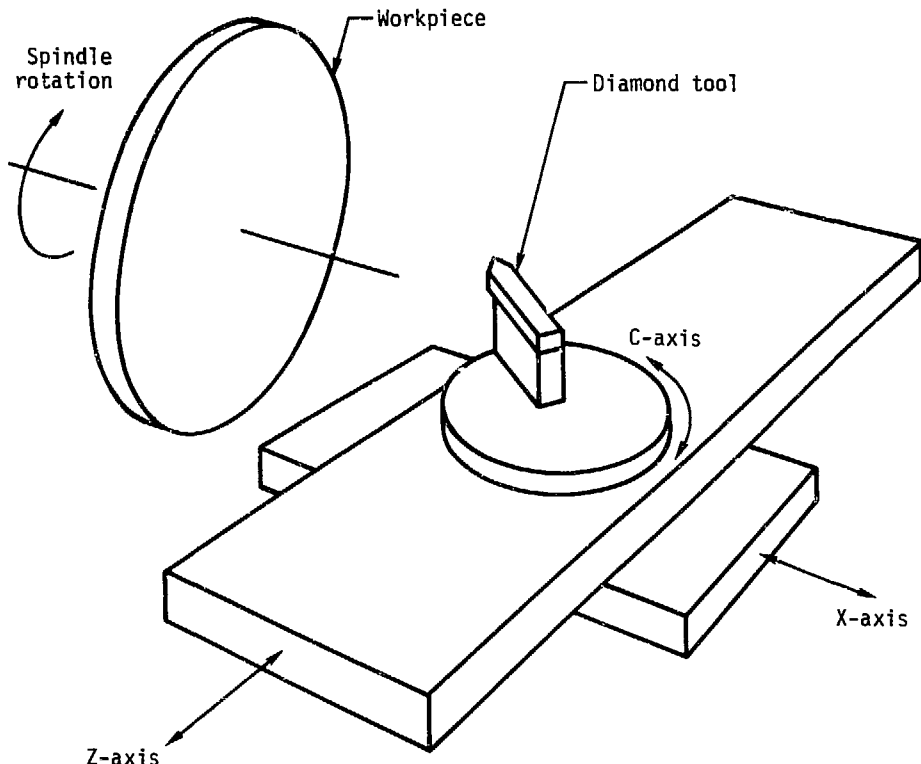


**Fig. 5.** The three axes of motion for the Moore diamond turning machine. The laser mirror being machined rotates about the spindle. The diamond tool moves toward the mirror along the Z-axis and across the mirror along the X-axis; it also rotates about the C-axis.

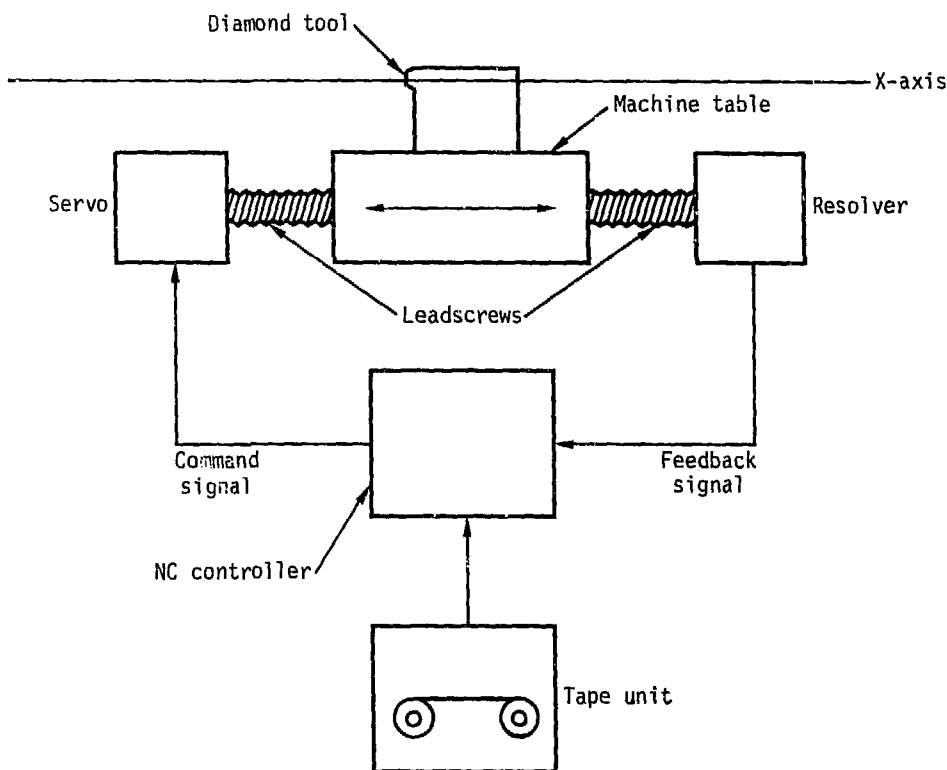


Fig. 6. The numerical control (NC) system used with LLL's Moore diamond turning machine. The control loop shown here controls machine motions along the X-axis.

employs either command pulses or feedback pulses (or, of course, both).

#### The Corrector Bar Hardware

The heart of the electronic corrector bar is an LLL-designed MCS-80 microcomputer. This is a modular, general-purpose microcomputer constructed on a number of standard-size printed circuit boards. The MCS-80 was selected because it had all the necessary capabilities and because it is in wide use and readily available at LLL, but any similar microcomputer would work equally well in this application. The MCS-80 includes the Intel 8080 central processing unit (CPU), necessary clock interrupt control, device decoders, input/output (I/O) port, memory, and power supplies. This particular application requires one 256-word page of random-access memory (RAM) and eighteen 256-word

pages of PROM to store the look-up table and the operating programs.

The corrector also includes three 254- $\mu$ m position counters (one each for the Z-, X-, and C-axes), the output interface logic needed to combine the command pulses from the NC controller and the correction pulses from the corrector, and a diagnostic correction display.

In operation, the corrector counts each command pulse in the NC controller (see Fig. 8). Each 10-mil position counter accumulates pulses for its particular axis, sends an interrupt signal to the microcomputer for each 13- $\mu$ m position change, and sets a flag at each 254- $\mu$ m position. If a 254- $\mu$ m position has been reached, correction pulses based on a correction word from the look-up table are sent to the output interface logic and distributed over the next 13- $\mu$ m motion at each 254- $\mu$ m position. The interface logic combines the

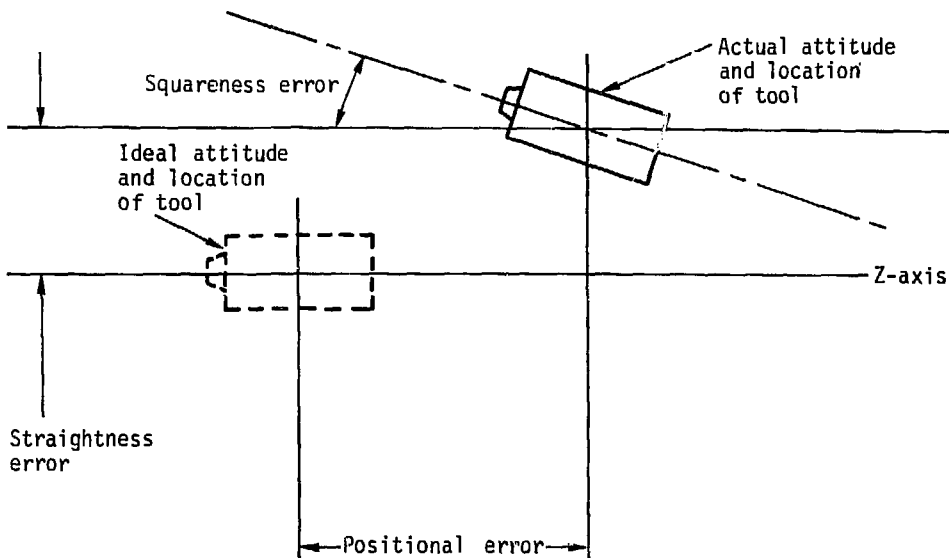


Fig. 7. Three machine errors. Only the motion of the diamond tool along the Z-axis is being considered. The errors are greatly exaggerated here for clarity.

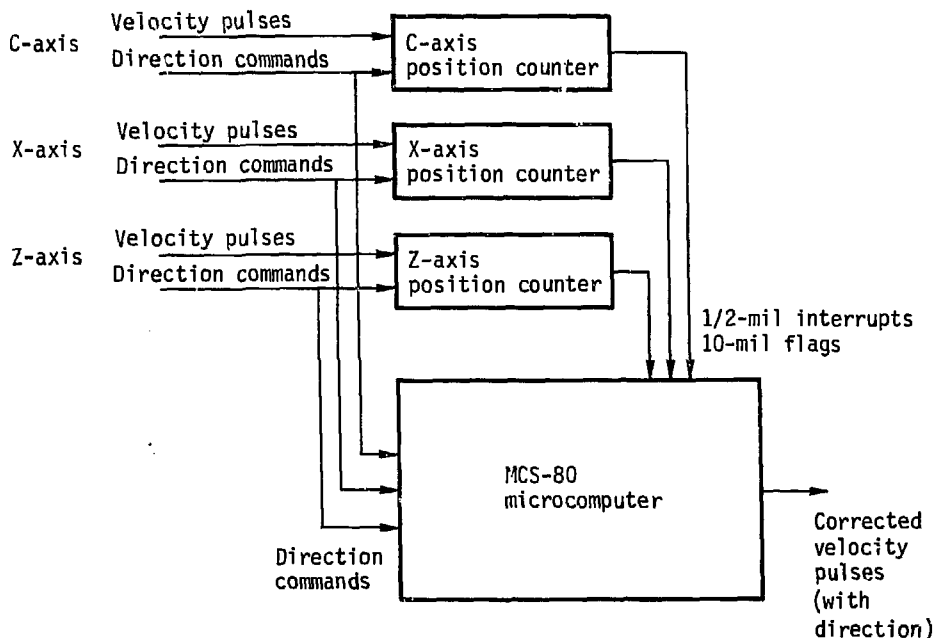


Fig. 8. Block diagram of the electronic corrector bar. The position counters count the command pulses from the NC controller and signal the microcomputer after each  $13 \mu\text{m}$  (1/2 mil) of machine displacement. After  $254 \mu\text{m}$  (10 mil) of machine displacement, the microcomputer inserts new corrected command pulses to the appropriate axis.

original NC command pulses with the correction pulses for each machine axis. The corrected command pulses consist of the NC command pulses during one time slot, position corrections during a second time slot, and straightness and squareness corrections during the last slot.

### **Results**

The corrector bar has performed at least as well as expected. The average surface roughness of a laser mirror that had been machined on the basic

numerically controlled diamond turning machine was  $0.4 \mu\text{m}$  (15  $\mu\text{in.}$ ) peak-to-peak (i.e., between highs and lows). Since the corrector has been incorporated into the system, the same mirrors are now being machined with an average roughness of  $0.1 \mu\text{m}$  (5  $\mu\text{in.}$ ) peak-to-peak.

A number of other NC machine tools at LLL will be upgraded by the addition of an electronic corrector bar. In fact, the corrector can be used to upgrade any NC machine tool that uses pulses in its command signals or in its feedback signals.

# A NEW X-RAY SPECTROMETER PROVIDES THE RECORDING SPEED NEEDED TO ANALYZE ELECTRON TEMPERATURES AND DENSITIES IN LASER-INDUCED PLASMAS

There are a number of applications where the photographic records of spectra produced by conventional x-ray spectrometers cannot be developed and analyzed quickly enough, or where the records may not even be recoverable. Developing speed was a problem in an application that uses an x-ray spectrometer to record and analyze data from laser-fusion experiments, which allow no more than an hour between successive shots. The problem has been overcome with an advanced x-ray spectrometer system that uses a self-scanning photodiode array to produce

*For further information on this article, contact Thomas J. Gadd (Ext. 8358).*

digital records of the low-energy x-ray spectra radiated by laser-fusion targets. The digital information is transmitted to a data-receiving system, where it is either analyzed immediately by a digital computer or stored on magnetic tape for later analysis.

## Introduction

An x-ray spectrometer system has been developed to record data from the low-energy spectra radiated by laser-fusion targets. The data being sought include the resonance and satellite lines of helium-like and hydrogen-like ionized silicon (see Fig. 9), which lie within the 1.8- to 2.2-keV energy range detected by the spectrometer. Once they have been recorded in

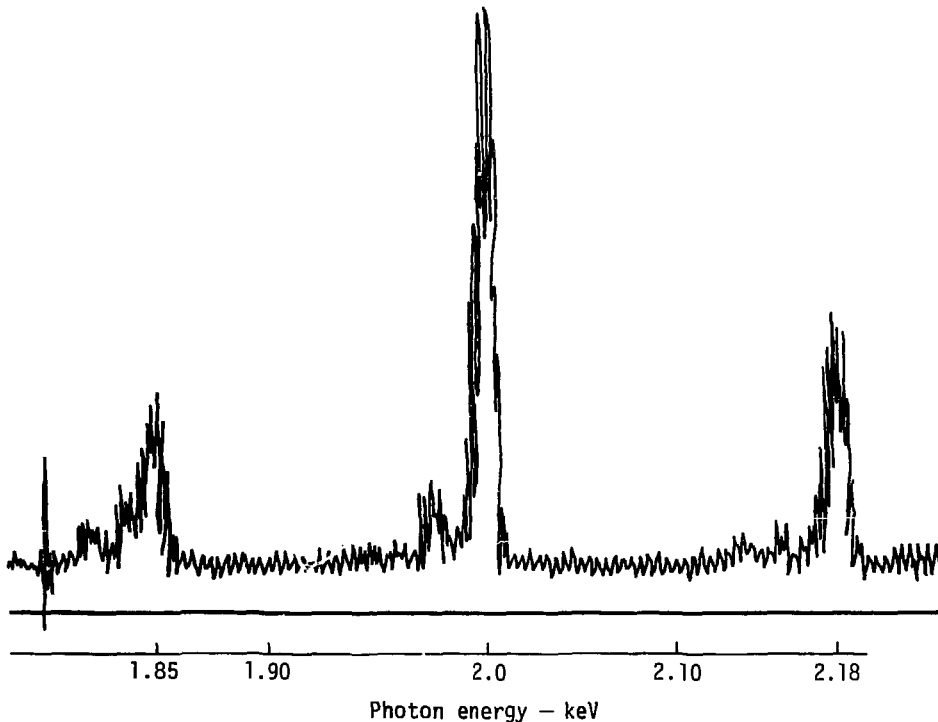


**Fig. 9.** A spectrogram made by the x-ray spectrometer. The spikes in the spectrum represent resonance lines produced by highly ionized silicon atoms in the plasma contained in the laser-fusion target.

x-ray spectrograms, these lines are measured and the results are used to deduce the electron temperature and density in the laser-induced plasmas that produced them. This information is a valuable aid in developing the method of inertial confinement of a controlled thermonuclear reaction.

In earlier x-ray spectrometers, spectra were recorded on photographic film. In the present system, spectral information is recorded and digitized by a self-scanning photodiode array. By eliminating the film, we avoid the tedious and time-consuming task of developing film, which must be completed in order to obtain a usable record.

In the laser application, experimental shots may be run as often as one every hour, and it's desirable to have the data processing completed from one test before going on to the next. In a second application that is still being developed, the spectrometer will be modified for use at the Nevada Test Site (NTS) to provide data useful in plasma diagnostics. In this case, recovery of film would be difficult or impossible, and environmental considerations such as shock arrival may necessitate data recovery within milliseconds.

In the new x-ray spectrometer, the 1024-element photodiode array records diffracted x rays either directly (in the laser-fusion application) or indirectly by means of light from a fluor being irradiated by x rays (the NTS application). The energies of the x rays of interest determine which of these two configurations will be used. As the photodiode array is scanned, its output is digitized, transmitted to a receiver, and stored in a microprocessor or on magnetic tape. The stored data are processed by either the microprocessor or a larger computer. The data can be displayed within 1 to 30 minutes — rather than hours, as in the case with film.

### **The Self-Scanning Photodiode Array**

The self-scanning photodiode array is a linear ensemble of 1024 P-N junction photodiodes built on a common silicon substrate (see Fig. 10). The center-to-center spacing of the photodiodes is 25  $\mu\text{m}$ . A logic network of transistors is built on the detector chip to scan and multiplex the signals from the photodiodes. The photodiode array has appreciable sensitivity to x rays with energies from 1.5 to above 10 keV, and the detector's response is a linear function of x-ray dose.

The signal levels from the photodiode array are processed at an analog sample rate of 100 kHz or greater by a sample-and-hold circuit. The photodiode array is allowed to run free without synchronization to the laser firing system. The photodiodes will store photocharges accumulated between consecutive scan cycles, so no data is lost if the laser event occurs at

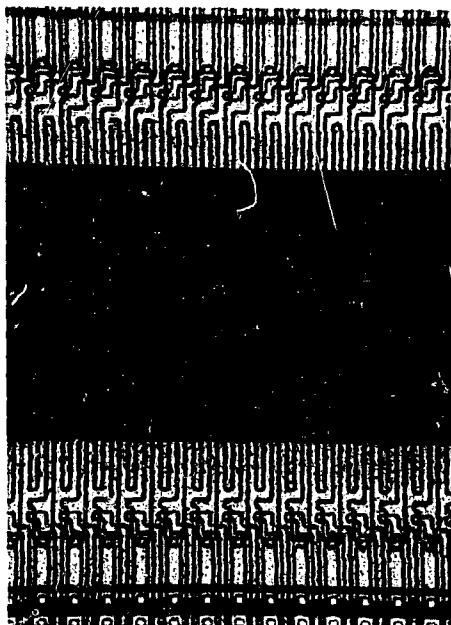


**Fig. 10.** Part of the surface of the self-scanning photodiode array. The width of the photosensitive area (along the fine lines) is 432  $\mu\text{m}$ .

an arbitrary point in a scan. The distribution of signal levels along the length of the photodiode array is reconstructed by a clock bit counter in the microprocessor system. The counter is actuated by an external event trigger.

### **System Description**

The spectrometer system has two primary groups of components: a detection group and a processing group. The detection group consists of a diffraction crystal, the photodiode detector already mentioned, a digitizer, and data-transmitting components. The processing group consists of a data receiver, data storage, and a computer with hardcopy and CRT display equipment.

The two groups are shown together in the schematic representations for the laser-fusion application (Fig. 11) and the NTS application (Fig. 12). The actual components used in the laser-fusion application are shown in Figs. 13 and 14.

In the laser-fusion application, x rays are allowed to fall onto a flat diffraction crystal of potassium acid phthalate (KAP) inclined at a 14° angle to the line

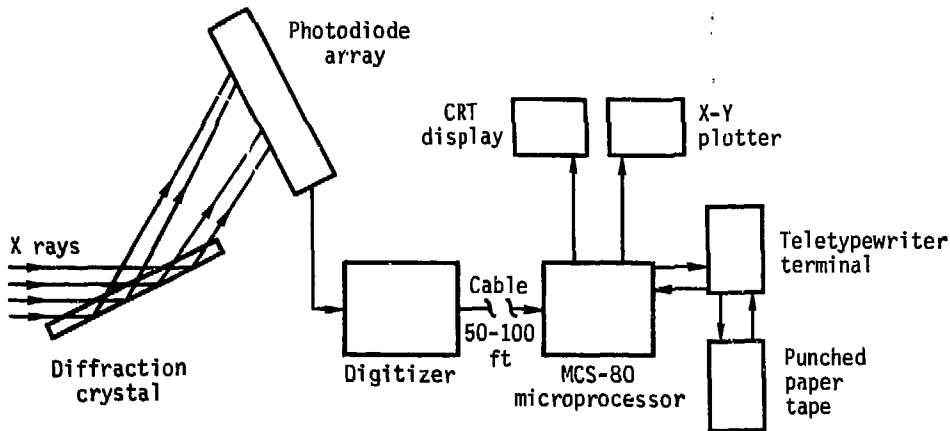


Fig. 11. Diagram of the x-ray spectrometer system used with laser-fusion experiments.

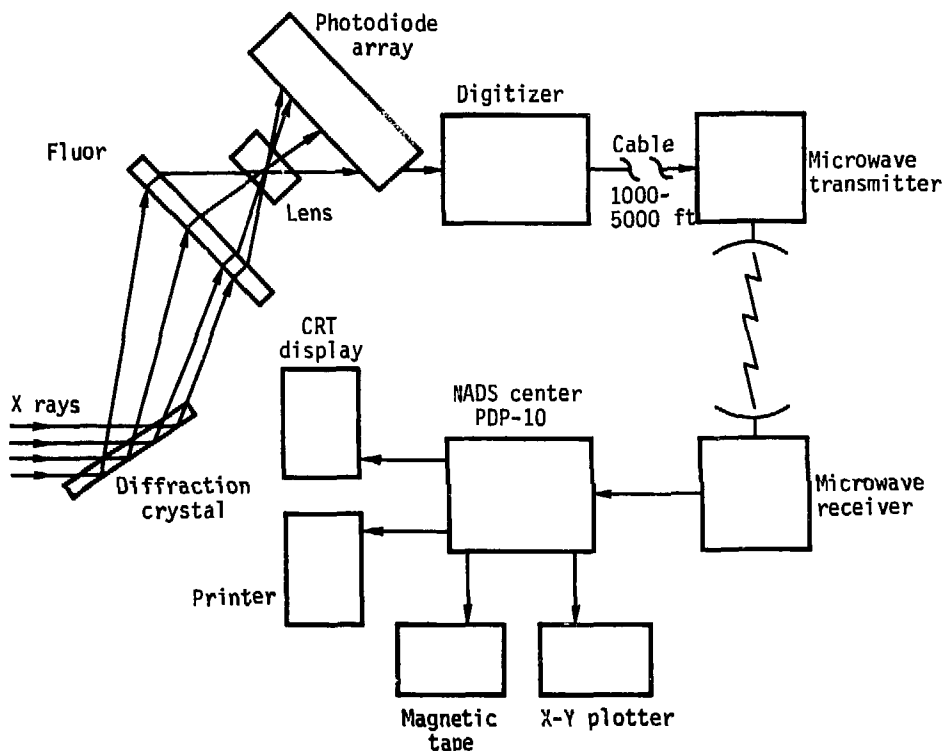
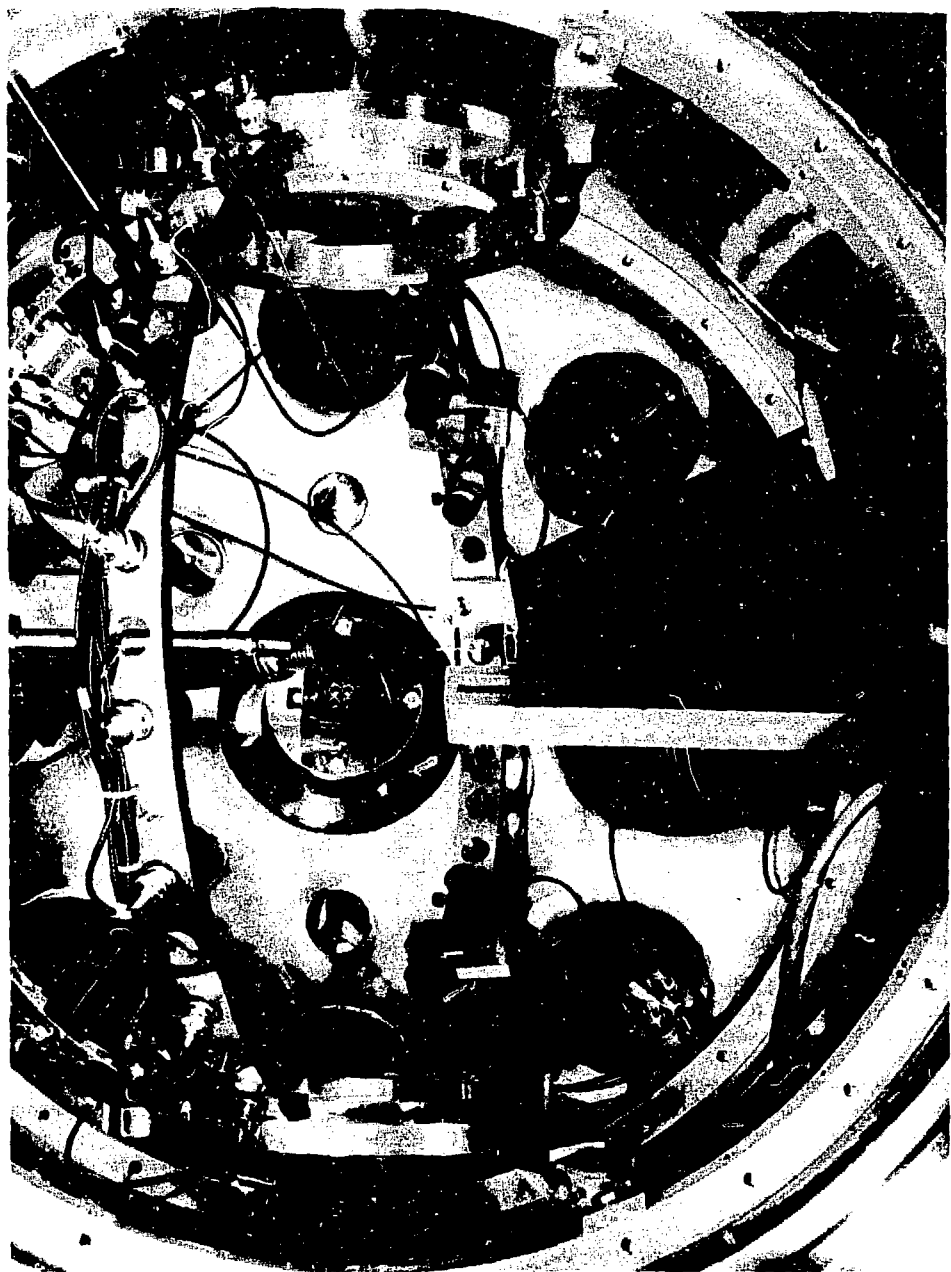


Fig. 12. Diagram of the x-ray spectrometer system modified for use at the Nevada Test Site.



**Fig. 13.** View showing the spectrometer installed inside a vacuum chamber for use with laser-fusion experiments. The diffraction crystal and the photodiode array are housed in the dark sloping box at the right. During laser shots, a target consisting of deuterium gas and tritium gas inside a tiny glass sphere is placed at the center of the vacuum chamber.



Fig. 14. The processing group used in laser-fusion experiments. The MCS-80 microprocessor is the top unit in the equipment rack. The CRT screen can be seen immediately below the microprocessor. The X-Y plotter rests on top of the equipment rack, and the teletypewriter with its paper-tape unit are just to the left of the rack.

of sight from the laser-fusion target. The x-ray spectrum reflected from the crystal is recorded by the 1024 elements in the photodiode array. The photodiode array is scanned and its analog output is digitized and transmitted over cables to the processing group, where an MCS-80 microprocessor stores and processes the data.

The hardware of the data system consists of the central processing unit (CPU), an array of direct-access solid-state memories, and several input/output (I/O) interfaces. The CPU, an Intel 8080, incorporates an 8-bit I/O data bus and a 16-bit memory bus. It can accommodate a memory as large as 64K words in direct access, and it can control up to 16 I/O devices. It has an instruction cycle time of 2  $\mu$ s. Our system provides 16K words of memory, of which 6.5K are given over to software. The remaining capacity is divided into four equal blocks to store the shot signals, the measured dark-current and offset levels, the sensitivity factors, and the reduced data.

To improve the quality of the data, the CPU also does some elementary arithmetic with the signal levels. Just before the laser shot, at the time the experiment

is enabled, the CPU has scanned and stored an array of dark-current and offset levels. These levels are subtracted from the event data. Also, the shot data are multiplied by predetermined factors that account for the variations in sensitivity from one photodiode element to another. The intensity resolution of the spectrometer data is improved to about one part in 250 by this processing.

After processing has been completed, an operator can distribute the reduced data and all segments of the raw data to any of a number of output media. The existing complement of I/O devices in the system includes a CRT display, an X-Y plotter, an IRIG clock, and an ASR-33 teletypewriter fitted with a paper tape punch and reader. The CRT display contains a 2048-word self-scanning memory, and it can display alphanumeric characters and plot line and bar graphs. The contents of the reduced data memory appear automatically on this unit immediately after a laser shot. Segments of the raw data can also be displayed if the operator wishes. The X-Y plotter is driven by an interface that includes two 12-bit digital-to-analog converters and a pen control circuit. The system software includes instructions that allow the plotter to be calibrated and scaled by the experimenter. Permanent numeric records, suitable for loading into a general-purpose computer, can be generated by the teletypewriter on punched paper tape. The records are labelled with IRIG time and written in scientific notation with four decimal digit resolution. The teletypewriter also serves as the communications terminal from which the operator types instructions to the microprocessor requesting data retrieval and output.

In the NTS application, the x-ray spectrum reflected from the diffraction crystal is aimed onto a fluor. The resultant light from the fluor is then focused onto the photodiode array. As the array is scanned, its analog output is digitized and stored in a temporary memory. Data in the memory is mixed with other information needed to reconstruct the data when it arrives at the processing group. The mixed data goes by cables to a microwave link that delivers it to the processing group.

The processing group in the NTS system is the Nevada Automated Diagnostics System (NADS) Center. Here the data is recorded on magnetic tape, and then read into a PDP-10 computer for processing. The processed data can then be printed out, plotted, displayed on a CRT screen, or written onto magnetic tape and delivered to the LLL computer center.

#### System Performance

The quality of the spectrograms produced by the new spectrometer compares favorably with the results

from film recordings. Signal-to-noise ratios are approximately 40:1, and they are expected to improve with future system modifications. In addition to its far greater data-processing speed and its convenience, the new system is not troubled by the false spectral

lines that are often produced by chemical agents used in the film method. Also, the use of a photodiode array to record spectra produces a detection system with a known and calibrated sensitivity, which is not always the case when spectra are recorded on film.

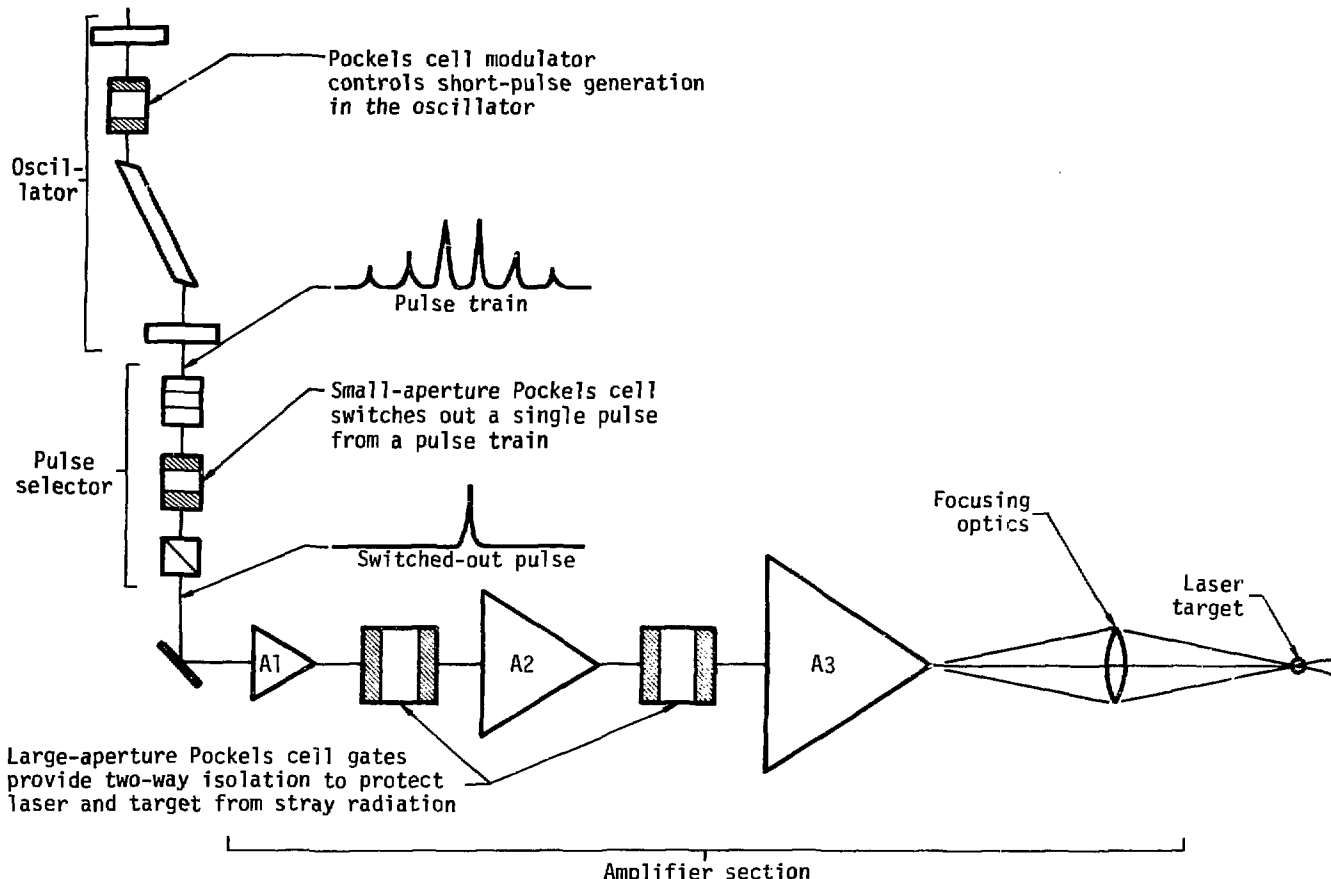


Fig. 15. Generalized schematic of a laser system that includes Pockels cells performing several different jobs.

# NEW DEVELOPMENTS IN ELECTROOPTIC MODULATOR TECHNOLOGY HAVE CREATED SPECIALIZED POCKELS CELLS THAT MEET THE DEMANDING REQUIREMENTS OF LASER SYSTEMS

The Pockels cell is an electrooptic device whose ability to modulate light pulses in laser beams has made it increasingly useful in sophisticated laser systems. In meeting the needs of the Laser-Fusion Program at LLL, two specialized Pockels-cell devices have been developed\* to provide the required switching speeds and contrast ratios. The first device, the ultrafast electrooptic modulator, provides optical gating and pulse shaping approaching intervals of  $10^{-10}$  s. The second device, the large-aperture Pockels-cell isolator, has been developed to achieve the necessary two-way optical isolation while minimizing the length of the device's crystal, which is very costly and time-consuming to grow.

## Introduction

A Pockels cell is an electronically controllable light modulator or optical switch. Polarized light passing through a clear electrooptic crystal in the cell is controlled by applying a voltage along the optical axis of the crystal. The Pockels cell (PC) has come to play an important role in laser systems because of this modulating and switching capability.

PC's can be used a number of ways in typical laser oscillator-amplifier systems, as Fig. 15 demonstrates. PC modulators can be used to produce short-duration, high-frequency pulses in laser oscillators. And as fast optical shutters, they can select a single output pulse from a train of ultrashort pulses. Although not indicated in Fig. 15, PC's may serve as optical gates, providing two-way isolation in a laser system to protect it from unwanted forward or backward radiation. PC's can also provide time shaping or amplitude- and/or phase-modulation control of laser radiation, tailoring the timing or frequency of input pulses in order to optimize the laser output pulse.

During the development of laser systems during the late 1960's and early 1970's, requirements arose for PC modulators whose performance characteristics were beyond the prevailing state of the art. In response, workers at LLL developed a new device geometry that improved both switching speed and contrast (on/off)

ratios, leading to two important PC modulators: the ultrafast electrooptic (EO) modulator and the large-aperture PC isolator. This work has been developed further for the requirements of present-day laser systems.

Improvements in switching speed have led to an ultrafast EO modulator capable of switching times in the subnanosecond range. To meet the fast pulse-amplitude and phase-modulation requirements, the optical gating and pulse-shaping operations must be done within intervals of approximately  $10^{-10}$  s. In practice, switching speeds have actually been improved by a factor of about 2 — from the previous limit of 0.5 to 1 ns down to 250 ps. More work will be required before the eventual goal of 100-ps switching times is achieved.

The device designed to provide improved contrast ratios, the large-aperture PC isolator, has been developed to produce two-way isolation for large-aperture (up to 50-mm diam) laser beams. The development of large-aperture PC devices is limited by the availability of large, high-optical-quality EO crystals. The special crystals used in such devices are very expensive and time-consuming to grow. Therefore, there is considerable advantage in designing for the minimum possible crystal size while still meeting or exceeding the important system requirements of contrast ratio, transmission uniformity, and switching speed. A number of design tradeoffs come into play, and the procedure that will be described in this article is the first systematic attempt at designing an optimum large-aperture EO device.

## Basic Pockels Cell Principles

The key element in the operation of the Pockels cell is the electrooptic crystal. The EO crystal employed in the LLL devices is a solution-grown potassium dideuterium phosphate ( $KD_2PO_4$  — or, more commonly,  $KD*P$ ) crystal of uniaxial (42m) symmetry. It has found many uses in high-power laser applications because of its excellent optical quality and high resistance to laser damage.

A representation of the  $KD*P$  crystal is shown in Fig. 16. The crystal is in the form of a right circular cylinder whose rotation axis is coincident with the optical (Z) axis of the crystal. Electrode bands of variable width and spacing are placed on the circumference of the cylinder as shown. When a

*For further information on this article, contact Bertram C. Johnson Jr. (Ext. 4359).*

\*The individuals who participated in this work were B. C. Johnson Jr., M. A. Summers, and K. R. Guign of the EE Department, and W. E. Martin and D. Milam of Y-Division.

potential is applied across the electrodes while a polarized light beam is passing through the crystal along the optical axis, the electrooptical effect in the KD\*P causes the light to experience a shift in polarization. The voltage required to shift the polarization direction by 90° is called the halfwave voltage  $V_\pi$ .  $V_\pi$  is approximately 7 kV in KD\*P for 1.06-μm light. As soon as the voltage is removed from the electrodes, the crystal no longer affects the polarization of the transmitted light. By placing a KD\*P Pockels cell between crossed polarizers, the amplitude of the transmitted light  $T$ , becomes a function of applied voltage  $V$ , according to the expression

$$T(V(r)) = T_0 \sin^2(\pi V/2V_\pi), \quad (1)$$

where  $T_0$  ( $0 \leq T_0 \leq 1$ ) accounts for losses due to

reflection, absorption, and scattering in the Pockels cell and polarizers.

### Design Considerations

The basic design problem for both the small, fast-switching modulators and the large-aperture Pockels cell isolators is to optimize certain important performance parameters. Device performance is optimized by varying the crystal geometry and electrode dimensions and designing the surrounding optical and electrical packaging of the crystal. For the small devices, the main performance parameter is switching speed, i.e., widest possible electrical bandwidth. For the large-aperture isolators, transmission uniformity across the aperture and the contrast (on/off) ratio are very important, while switching speed is a secondary consideration. The extent to which device performance has been

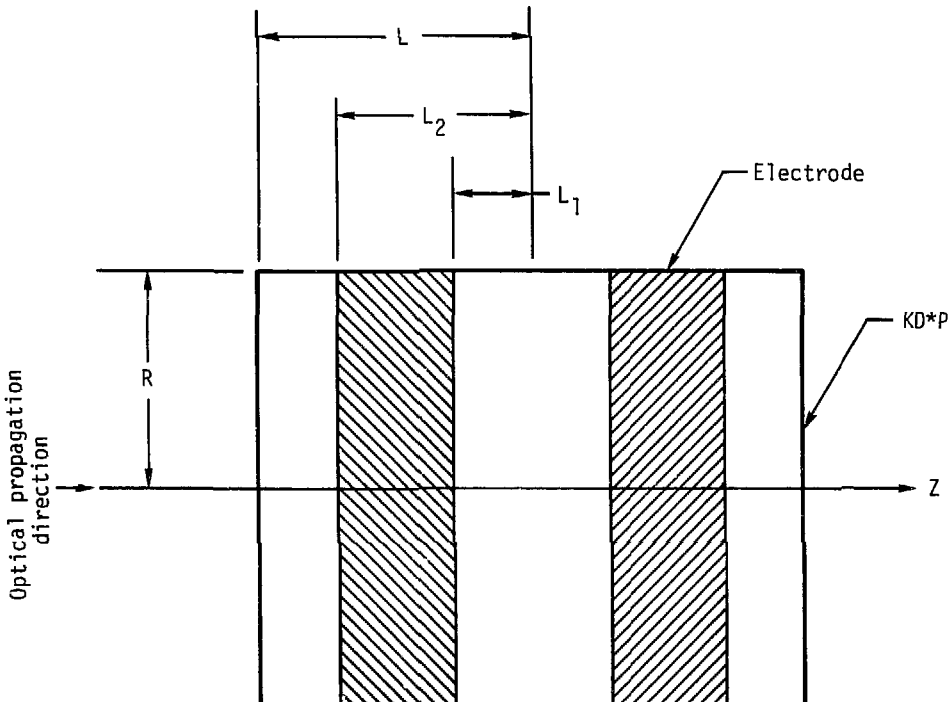


**Fig. 16.** The cylindrical ring-electrode (CRE) Pockels cell. The Z-axis of the cylindrically shaped crystal of KD\*P is both the optical axis of the crystal and the axis of the cylinder. The variables  $R$ ,  $L$ ,  $L_1$ , and  $L_2$  are chosen carefully to produce the desired operating characteristics.

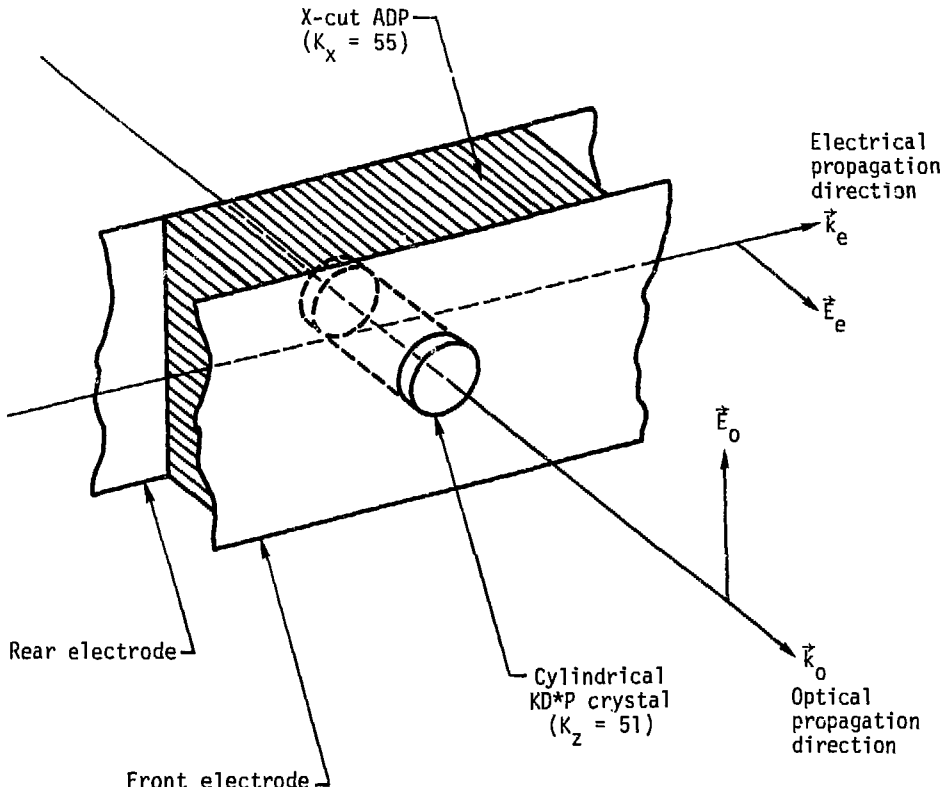


Fig. 17. The ultrafast Pockels-cell modulator. The KD\*P crystal is mounted in a parallel-plate stripline whose ammonium dihydrogen phosphate (ADP) dielectric material provides a close match to the dielectric constant of the KD\*P.

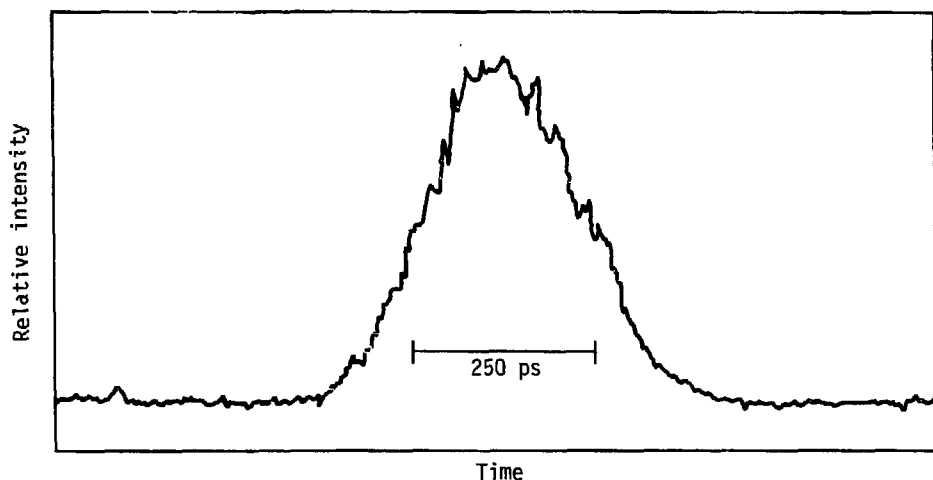
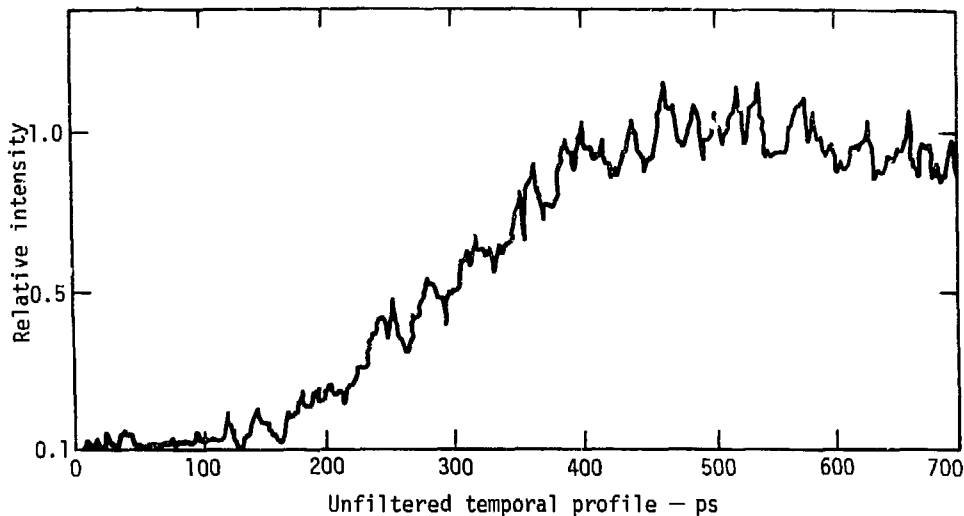
optimized will be discussed in the following sections, along with the associated tradeoffs and design constraints.

#### Ultrafast Pockels Cell Modulators

The crystal selected for the ultrafast EO modulator is represented in Fig. 16. It is 3 mm in diameter ( $R = 1.5$  mm) and 7 mm long ( $L = 3.5$  mm).  $L_1$ , the distance from crystal center to electrode inner edge, was 2.5 mm and  $L_2$  was 3.5 mm (i.e., the electrode outer edge was at the end of the crystal). The capacitance of this configuration is approximately 0.65 pF, which, when driven by a  $50\text{-}\Omega$  transmission line, would be expected to exhibit an RC risetime of about 70 ps.

By placing the crystal in a parallel-plate stripline that is impedance matched as closely as possible to the  $50\text{-}\Omega$  driving circuitry, it is possible to run the device

as a transmission line (see Fig. 17). Furthermore, by using a dielectric material in the stripline that closely matches the dielectric constant of the KD\*P crystal, the entire unit behaves as a transmission line, with distributed inductance and capacitance. In the ideal limiting case, the switching time of the device is limited only by electrical and optical transit times through the crystal. For the device in Fig. 17, the electrical transit time across the crystal diameter is about 70 ps. For a 1-mm-diam input beam we would expect a purely transit-time-limited device to respond in approximately 40 ps. In the actual device, however, a number of factors tend to limit the experimentally observed risetimes to values considerably longer than the transit time limit. The primary limitation is the electrical design and construction of the Pockels cell. Here, frequency dispersion, attenuation, and voltage reflections due to imperfect impedance matching act



(b) Risetime = 250 ps with shorting stub

**Fig. 18.** The risetimes for two prototype ultrafast Pockels-cell modulators. (a) The 260-ps risetime for this feedthrough stripline device was consistent with theoretical expectations. (b) The second device, which included a shorting stub close to the crystal, gave a 250-ps pulse output.

in concert to limit the actual risetime values to the range of 200 to 500 ps or longer.

Risetime data for two prototype devices are shown in Fig. 18. In the first case (Fig. 18(a)), there was a typical 10 to 90% optical transmission rise of 260 ps for a feedthrough stripline device, which was consistent with the number estimated by folding the  $\sin^2 V$  transmission dependence (see Eq. 1) into the 300-ps voltage risetime response observed in an earlier small-signal sampling measurement.

The second curve (Fig. 18(b)) shows the results for a special case where the PC incorporated a shorting stub very close to the crystal. A comparable risetime was obtained — about 250 ps. In this case the stub reflects the incident voltage pulse back on itself with a change of polarity, and the optical pulse is quickly terminated. Thus, a pulse is produced whose full width at half maximum is approximately 250 ps. This pulse is the shortest optical pulse produced by a Pockels cell to date. This short pulse was possible because of the electrical length of the shorting stub at the end of the crystal, which caused the applied voltage pulse to be reflected back through the crystal before it had time to reach its maximum (halfwave) value. This means that the price paid for the short pulse was a reduction in transmission or, alternatively, an increased insertion loss through the device. For the case of Fig. 18(b), the fraction of input pulse intensity transmitted through the shorted stub cell was estimated to be on the order of 1 to 5%.

A summary of risetime measurements on a number of devices is listed in Table 1. These risetimes are at or slightly ahead of the state of the art for devices capable of withstanding high power fluxes and exhibiting high contrast ratios. In terms of the objectives of the Laser-Fusion Program at LLL, these results suggest that the Pockels cell may prove useful in generating special time-shaped pulses that are

Table 1. Pockels cell risetimes (10 to 90%) for KD\*P stripline devices

Device	Electrical risetime (ps)	Optical risetime (ps)
10-mm-aperture cell	525	450
7-mm-aperture cell	260	—
3-mm-aperture cell	300	330
3-mm-aperture cell <sup>a</sup>	300	260
3-mm-aperture cell with shorted stub	210 <sup>b</sup>	250

<sup>a</sup>A different high-voltage (spark gap) driver was used.

<sup>b</sup>This is the round-trip time (electrical) of the shorted stub.

optimally suited to producing thermonuclear reactions in small target pellets.

#### Large-Aperture Pockels-Cell Isolators

To satisfy the requirement for effective bidirectional isolators for the Shiva laser, a 50-mm clear-aperture Pockels cell was needed with a transmission uniformity of better than 2% across the full aperture. A reasonable driving voltage ( $\leq 10$  kV) and the fastest possible risetime ( $\leq 10$  ns) were also required, but the primary design objective was to minimize the size of the KD\*P crystal in order to minimize the contribution of the Pockels cell to nonlinear phase distortion and improve the contrast ratio by reducing strain-induced birefringence intrinsic to large crystals. Besides decreasing the cost, minimizing the amount of crystal material would not only tend to improve the device contrast ratio, but also considerably shorten the delivery time of the 20 large-aperture devices needed for Shiva. In fact, it was apparent that the volume of high-optical-quality material required for the twenty 50-mm devices and twenty-one smaller (25-mm) devices would severely tax the KD\*P crystal-growing capacity of the United States for the next year!

The cylindrical ring-electrode (CRE) Pockels cell designed at LLL satisfied most of our objectives, and it became the starting point for the design of large-aperture devices. It was clear that by scaling this geometry ( $L/R = 2$  from Fig. 16) to meet the clear-aperture requirements, a usable 50-mm-diam Pockels cell could be built if large, high-quality KD\*P crystals were available in sufficient quantities. These crystals grow along the Z axis at rates that vary between 0.1 mm and 1 mm per day, depending on deuteration level and growing technique. If the CRE geometry were scaled at  $L/R = 2$ , then 3700 mm of KD\*P Z length would be needed for Shiva. Because of the time required to grow this much material, a method was sought to reduce the crystal length, i.e., using a design with  $L/R < 2$ .

The catch was that calculations indicated a reduction in the crystal length would result in an unacceptable loss in transmission uniformity. It seemed possible, however, that a slight modification to the electrode geometry might allow the loss in transmission uniformity to be recovered at the expense of an increase in driving voltage. An analysis of the electrode geometry was made based on the fundamental relationship given by Eq. 1 for the transmission of the EO crystal between crossed polarizers as a function of applied voltage. In general,  $V$  in Eq. 1, the radius-dependent voltage between crystal faces, is some fraction of the voltage applied to the electrode. This radial dependence is caused by the electric field fringing effects of the CRE geometry. Spatial

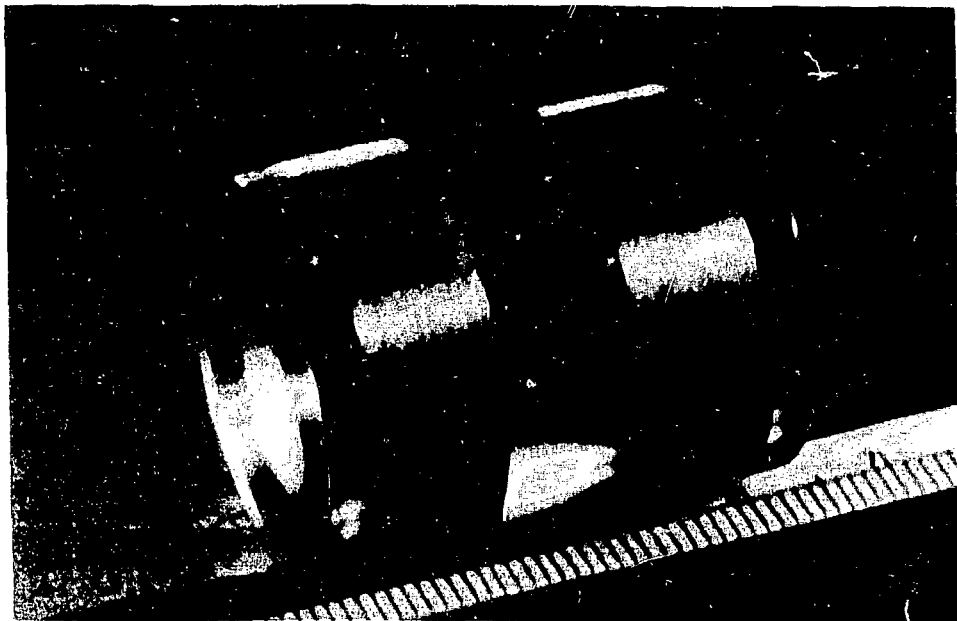


Fig. 19. The KD\*P crystal used to verify the voltage-distribution calculations for the large-aperture Pockels-cell isolator. (Scale is graduated in mm.)

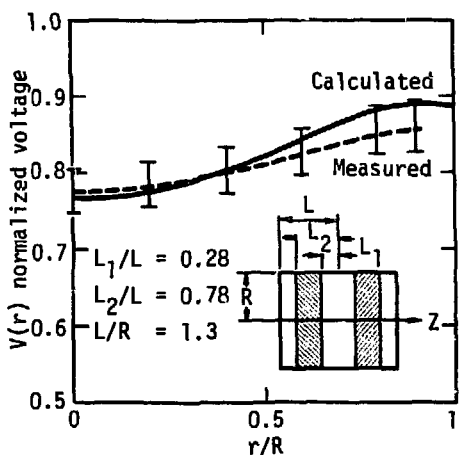


Fig. 20. The voltages obtained with the prototype large-aperture device correspond closely with the predicted values.

nonuniformities in transmission through the polarizer-crystal-polarizer combination resulting from the radial variations in voltage were minimized and traded against voltage coupling, i.e., the ratio of voltage between crystal faces to the electrode voltage (see Fig. 16).

Radial voltage distributions were calculated by means of a numerical solution to the Laplace equation for several electrode geometries in which electrode position, electrode width, and crystal size ( $L/R$ ) were varied systematically. Results from computer simulations were summarized graphically, and an optimum electrode geometry and crystal size were chosen. The results showed that acceptable transmission uniformity and voltage coupling could be achieved using a cylindrical crystal with  $L/R = 1.3$ . This ratio reduced the  $Z$  length by 35% (volume reduction), shortened the delivery time, and improved the contrast ratio. A prototype was built and tested to verify the voltage calculations (see Fig. 19). The test (prototype) crystal performed as predicted, as shown in Fig. 20, which gives a comparison between

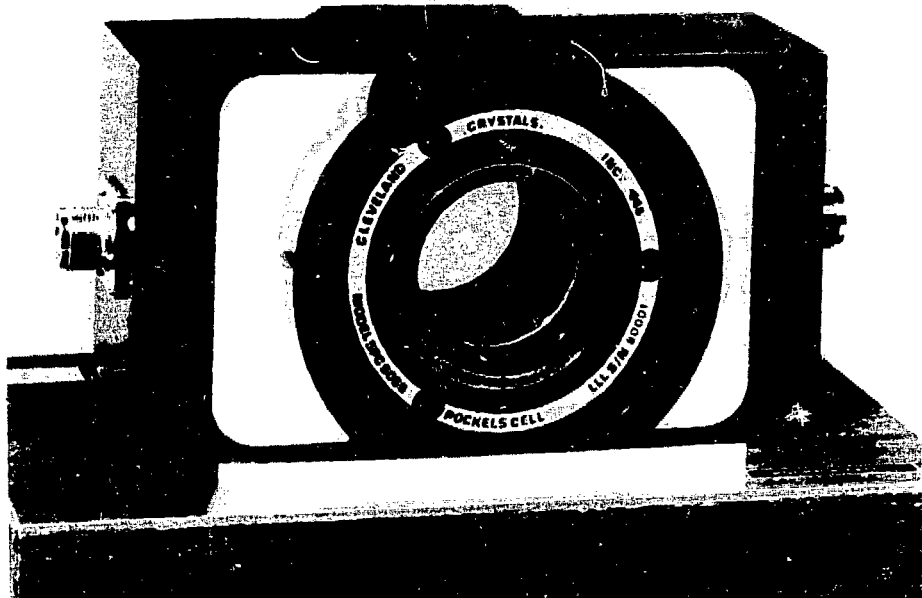


Fig. 21. The completed large-aperture Pockels-cell isolator enclosed in an aluminum housing.

the measured and calculated values of  $V(r)$  normalized to the electrode voltage.

A complete assembly of a prototype device is shown in Fig. 21. The crystal is enclosed in an aluminum housing with protective glass windows. This device yielded an even closer match to the calculated values of  $V(r)$  than expected. The transmission uniformity of this Pockels cell between crossed polarizers will be better than 2% peak-to-valley for an applied electrode voltage of  $1.2 V_{\pi}$ , or less than 10 kV pulsed at  $\lambda = 1.06 \mu\text{m}$ .

Switching time for the device will be less than 10 ns using a driver with a  $50\text{-}\Omega$  source impedance. Faster risetimes could be achieved by reducing this impedance. The intrinsic contrast ratio of the complete assembly shown in Fig. 21 was measured to be 250:1

at  $\lambda = 0.6328 \mu\text{m}$ . This means a value of approximately 700:1 can be expected at  $\lambda = 1.06 \mu\text{m}$ . Strain effects would probably have prevented this high contrast ratio from being achieved if the crystal were longer, i.e., if  $L/R > 1.3$ .

The reduction in crystal length from 10 cm at  $L/R = 2$  to 6.5 cm at  $L/R = 1.3$  has made the 50-mm, clear-aperture Pockels cell practical in the unprecedented quantities required for the Shiva laser system.

#### Acknowledgments

Acknowledgment is gratefully given for the contributions to this work made by D. Roberts of Cleveland Crystals, Inc. and D. Anafi of Lasermetrics, Inc.